Supporting Information

for *Adv. Funct. Mater.,* DOI: 10.1002/adfm.201700860

Band-Tail Recombination in Hybrid Lead Iodide Perovskite

*Adam D. Wright, Rebecca L. Milot, Giles E. Eperon, Henry J. Snaith, Michael B. Johnston, and Laura M. Herz**

Supporting Information

Title Band-tail Recombination in Hybrid Lead Iodide Perovskite

*Adam D. Wright, Rebecca L. Milot, Giles E. Eperon, Henry J. Snaith, Michael B. Johnston, and Laura M. Herz**

Contents

A. Functional form of fits to PL transients

The dynamics of charge-carrier recombination can be described by the following rate equation:

$$\frac{\mathrm{d}n}{\mathrm{d}t} = -k_3 n^3 - k_2 n^2 - k_1 n \tag{S1}$$

where n is the charge-carrier density, k_1 is the decay constant for monomolecular decay processes such as trap-mediated recombination, k_2 is the bimolecular (electron-hole) recombination rate constant and k_3 is the Auger recombination rate constant.[1]

At lower excitation densities, monomolecular recombination dominates. The monoexponential function $I_{\mathrm{me}}(t) = I_0 e^{-k_1 t}$, commonly[2] used to fit photoluminescence (PL) transients, arises from neglecting the bimolecular and Auger terms in Equation (S1), and taking the PL intensity $I_{\mathrm{me}}(t)$ to be proportional to n. I_0 is the PL intensity at $t = 0$. A biexponential function $I_{\mathrm{be}}(t) = I_1 e^{-t/\tau_1} + I_2 e^{-t/\tau_2}$ may instead be used to account for both a fast and a slow monomolecular decay component, attributable to separate populations of charge carriers.[3] A stretched exponential function $I_{\mathrm{se}} = I_0 e^{-(t/\tau_{\mathrm{c}})^{\beta}}$ has also been used to phenomenologically account for the presence of a local distribution of monoexponential decay rates.[4] Here, a more heterogeneous distribution of decay rates corresponds to a distribution coefficient, β, which is closer to 0 than 1, while the time taken for the PL intensity to drop to I_0/e is τ_{c}, the characteristic lifetime.[4a]

Alternatively, bimolecular recombination may be taken into account as well.[5] If only the Auger recombination term is neglected, integration of Equation (S1) yields:

$$n_{bm}(t) = \frac{k_1}{k_2}\left[e^{k_1 t}\left(1 + \frac{k_1}{n_0 k_2}\right) - 1\right]^{-1} \tag{S2}$$

where n_0 is the initial charge-carrier density.

The sum of many monoexponential decays with densely distributed lifetimes τ_i, $I(t) \sim \sum_i e^{-t/\tau_i}$, approximates to a power-law decay[6] with exponent α, i.e. a function of the form $I_{\mathrm{pl}}(t) = I_0 t^{-\alpha}$ as detailed in Section B of the Supporting Information.

The following procedures were used to obtain the fits to the 10 K PL transient depicted in Figure 1b of the main text:

- $I_{\mathrm{me}}(t)$ was fitted between 20 and 100 ns, over which the data appeared to follow a roughly linear trend when depicted on a logarithmic intensity scale, resulting in $k_1 = 1.96 \times 10^6$ s^{-1}.

- $I_{\mathrm{be}}(t)$ was fitted between 1 and 100 ns, beyond which the fit did not converge well. The resultant decay lifetimes were $\tau_1 = 2.22$ ns and $\tau_2 = 39.8$ ns.

- $I_{\mathrm{se}}(t)$ was fitted to the data up to 1 µs, beyond which the fit did not converge well. The fit converged with β=0.1939 and τ_{c}=1.51× 10^{-2} ns.

- With k_2 fixed at 10^{-10} cm^3 s^{-1},[1] Equation (S2) was fitted between 1 ns and 100 µs, beyond which the fit did not converge well. The fit converged with $k_1 = 2.21 \times 10^4$ s^{-1} and n_0 at its upper bound of 10^{18} cm^{-3}.

- $I_{\mathrm{pl}}(t)$ was fitted to the data over the entire time range, with α = -1.027 ± 0.003. For the 20 and 30 K data, α = -1.071 ± 0.004 and -1.19 ± 0.01 respectively.

B. Power-law time dependence of PL

Power-law decays take the form $I(t) \propto t^{-\alpha}$, where I is intensity, t is time and α is some positive constant, and result from the superposition of many monoexponential decays with densely-distributed recombination rates.[6a, 7] Several models have been developed to explain the physical origin of power-law decays for luminescence[7a, 8]. A common feature is that charge-carriers are localized in trap states with an occupation probability $p(t)$ of the form $p(t) = e^{-\gamma t}$, where the functional form of the escape rate γ varies with the model.[9] The models can be divided into two categories, in which the escape rate depends on either the energetic depth of the traps (Arrhenius detrapping models) or the separation between traps (hopping models). In both cases, the total PL intensity can be shown analytically to decay as a power law, given certain reasonable assumptions.

Arrhenius detrapping models

In Arrhenius detrapping models, the escape rate from a trap of energetic depth ε has the form

$$\gamma_{\mathrm{Arr}}(\varepsilon) = \nu_0 e^{-\varepsilon/k_{\mathrm{B}}T} \tag{S3}$$

where ν_0 is the attempt-to-escape frequency.[9] The PL intensity decays as a power law if the energetic distribution of the traps is exponential.[8a, 10]

In the simplest such model the charge-carrier is assumed to rapidly undergo radiative recombination after escaping to the band edge, without retrapping.[11] Randall and Wilkins[8a, 11] analytically derive a power-law decay under these conditions as follows:

If $N(\varepsilon,t)$ is the number of charge-carriers in traps of depth ε at time t, then

$$\frac{\mathrm{d}N(\varepsilon,t)}{\mathrm{d}t} = -N(\varepsilon,t)\gamma_{\mathrm{Arr}}(\varepsilon) \tag{S4}$$

Integrating then gives

$$N(\varepsilon,t) = N_0(\varepsilon)\exp\left(-\nu_0 t e^{-\varepsilon/k_{\mathrm{B}}T}\right) \tag{S5}$$

where $N_0(\varepsilon) = N(\varepsilon,0)$. The PL intensity $I(t)$ is proportional to the rate of supply of charge-carriers to the band edge, so if the traps have an energetic distribution given by $n(\varepsilon)$,

$$I(t) \propto \int_0^\infty n(\varepsilon)\frac{\mathrm{d}N(\varepsilon,t)}{\mathrm{d}t}\mathrm{d}\varepsilon \tag{S6}$$

Thus, for an exponential energetic distribution of traps with characteristic depth ε_0, $n(\varepsilon) = Ae^{-\varepsilon/\varepsilon_0}$, and assuming $N_0(\varepsilon) \propto n(\varepsilon)$,

$$I(t) \propto \int_0^\infty Ae^{-\varepsilon/\varepsilon_0}\exp\left(-\nu_0 t e^{-\varepsilon/k_{\mathrm{B}}T}\right)\nu_0 e^{-\varepsilon/k_{\mathrm{B}}T}\mathrm{d}\varepsilon \tag{S7}$$

Substitution of $\xi = \nu_0 t e^{-\varepsilon/k_{\mathrm{B}}T}$ yields

$$I(t) \propto A\frac{k_{\mathrm{B}}T}{t}(\nu_0 t)^{-k_{\mathrm{B}}T/\varepsilon_0}\int_0^{\nu_0 t}\xi^{-k_{\mathrm{B}}T/\varepsilon_0}\exp(-\xi)\,\mathrm{d}\xi \tag{S8}$$

The upper limit of the integral may be taken to infinity since for typical observation times, $t \gg \nu_0$. Therefore $I(t) \propto t^{-(1+k_{\mathrm{B}}T/\varepsilon_0)}$, a power law decay.[8a]

The multiple-trapping model is a more sophisticated Arrhenius detrapping model, in which charge-carriers are permitted to be repeatedly excited to, and retrapped from, the band-edge.[10b] Orenstein and Kastner[10b] describe how multiple-trapping causes the transient photocurrent to exhibit power-law kinetics. Their formalism can also be applied to the PL by considering activation to the band edge rather than the mobility edge.

Hopping models

In the case of hopping models, trapped charge-carriers tunnel between localized traps spatially separated by distance r at a rate[9, 12]

$$\gamma_{\mathrm{hop}}(r) = Ae^{-r/R_0}, \tag{S9}$$

$$\begin{aligned} A &= \nu_0 e^{-\Delta\varepsilon/k_B T} \text{ for } \Delta\varepsilon > 0 \\ &= \nu_0 \text{ for } \Delta\varepsilon < 0 \end{aligned}$$

where R_0 is the decay length of the charge-carrier wavefunction and A is a prefactor containing the frequency of escape attempts ν_0 and the difference in energy between the destination and origin sites for the hopping, $\Delta\varepsilon$.

Huntley[7a] uses a model in which one sign of charge carrier is mobile, to derive an approximate power law decay for the case when the traps are randomly distributed in space. In an analogous fashion to Equation (S6), the PL intensity $I(t)$ in these models is proportional to the rate at which oppositely-charged carriers tunnel together, so

$$I(t) \propto \int_0^\infty p(r)\frac{\mathrm{d}N(r,t)}{\mathrm{d}t}\mathrm{d}r \tag{S10}$$

where $p(r)$ is the probability that such a recombining pair of carriers are in traps separated by r and $N(r,t)$ is the number of such pairs separated by r at time t. Charge-carriers are assumed to recombine with their nearest eligible neighbour, and A is assumed to be constant.

For recombination centres randomly distributed in space, the probability of a recombination centre being within a volume V of a trapped carrier follows the exponential distribution, with probability density $p(V) = \rho e^{-\rho V}$. The probability that the nearest recombination centre lies between a distance of r and r+dr of the trapped carrier is therefore

$$p(r)\mathrm{d}r = e^{-\frac{4}{3}\rho\pi r^3}4\pi\rho r^2\mathrm{d}r \tag{S11}$$

By the same steps as expressed in Equations (S4) to (S7), we arrive at

$$I(t) \propto \int_0^\infty e^{-\frac{4}{3}\pi\rho r^3}4\pi\rho r^2 \exp\left(-Ate^{-r/R_0}\right)Ae^{-r/R_0}\,\mathrm{d}r \tag{S12}$$

Assuming that most electrons recombine around their mean lifetime $1/\gamma_{\mathrm{hop}}(r)$, at a given time t then all electrons within a distance r_c of a recombination centre will have tunnelled there, where

$$t = \frac{1}{\gamma_{\mathrm{hop}}(r_c)} = A^{-1}e^{r_c/R_0}, \tag{S13}$$

$$r_c = R_0\ln(At)$$

Then the integral in Equation (S12) reduces to only the case when $r=r_c(t)$, so

$$I(t) \propto e^{-\frac{4}{3}\pi(R_0\ln(At))^3}4\pi\rho R_0^3(\ln(At))^2 t^{-1} \tag{S14}$$

This approximates to t^{-1} provided the density of recombination centres is not too large relative to the volume of the charge-carrier wavefunction ($\rho \ll \frac{4}{3}\pi R_0^3$).

In Dunstan's model of distant-pair recombination, the possibility that an electron's nearest neighbour hole may recombine with its own nearer neighbour electron is also accounted for.[8b] This complicates the form of $p(r)$, but still produces power-law PL decays.

C. Time dependence of PL spectra at different temperatures

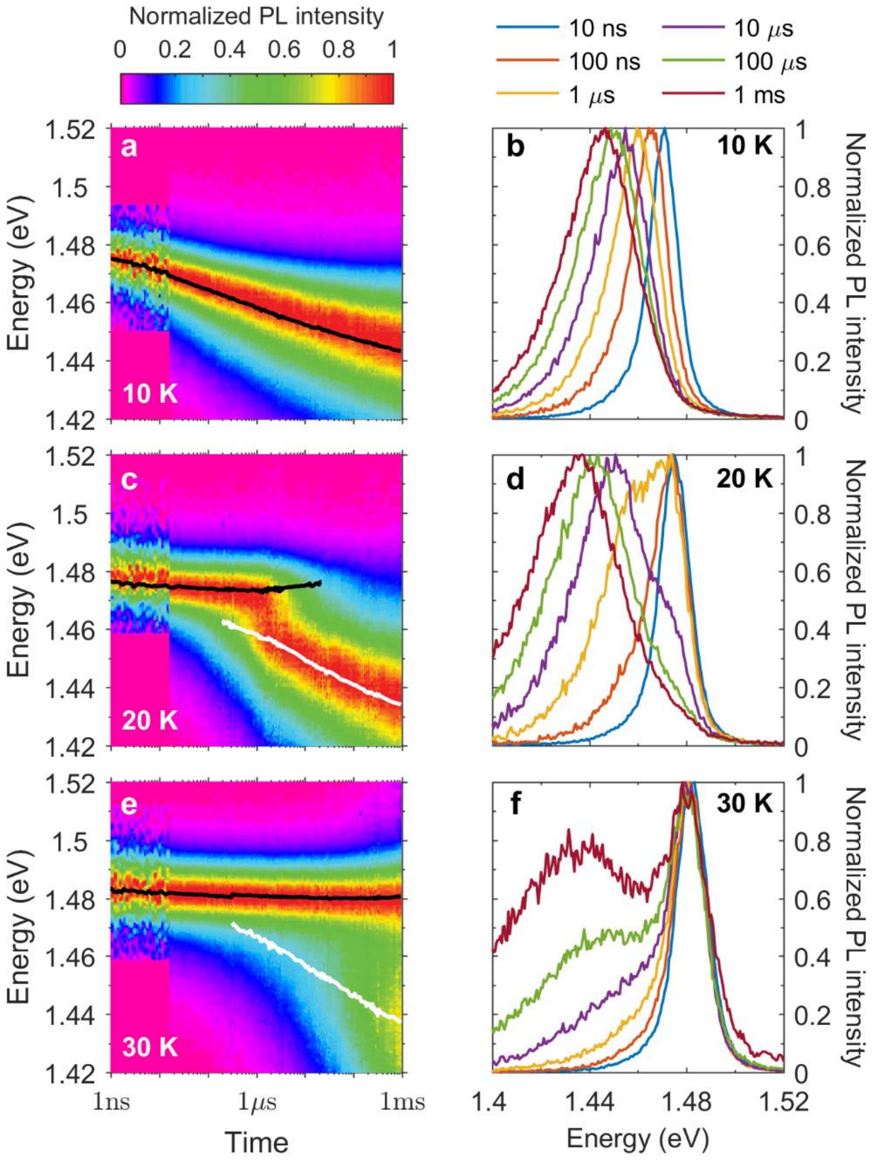

Figure S1. Color plots of the normalized time-dependent PL spectra of $FAPbI_3$ at times between 1 ns and 1 ms and under an excitation fluence of 390 nJ/cm^2, with selected spectra, at temperatures of **(a,b)** 10 K, **(c,d)** 20 K and **(e,f)** 30 K. The spectra were fitted with one or two Gaussian peaks, whose central energies are indicated by the solid black and white lines.

D. Temperature dependence of PL at different excitation fluences

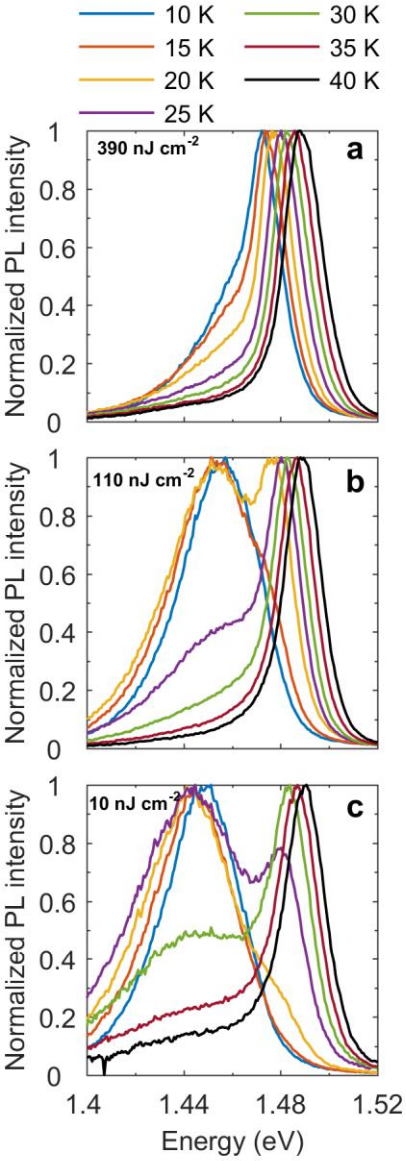

Figure S2. Time-integrated PL spectra at selected temperatures for $FAPbI_3$ under excitation fluences of **(a)** 390 nJ/cm^2, **(b)** 110 nJ/cm^2 and **(c)** 10 nJ/cm^2.

E. Power dependence of PL at different temperatures.

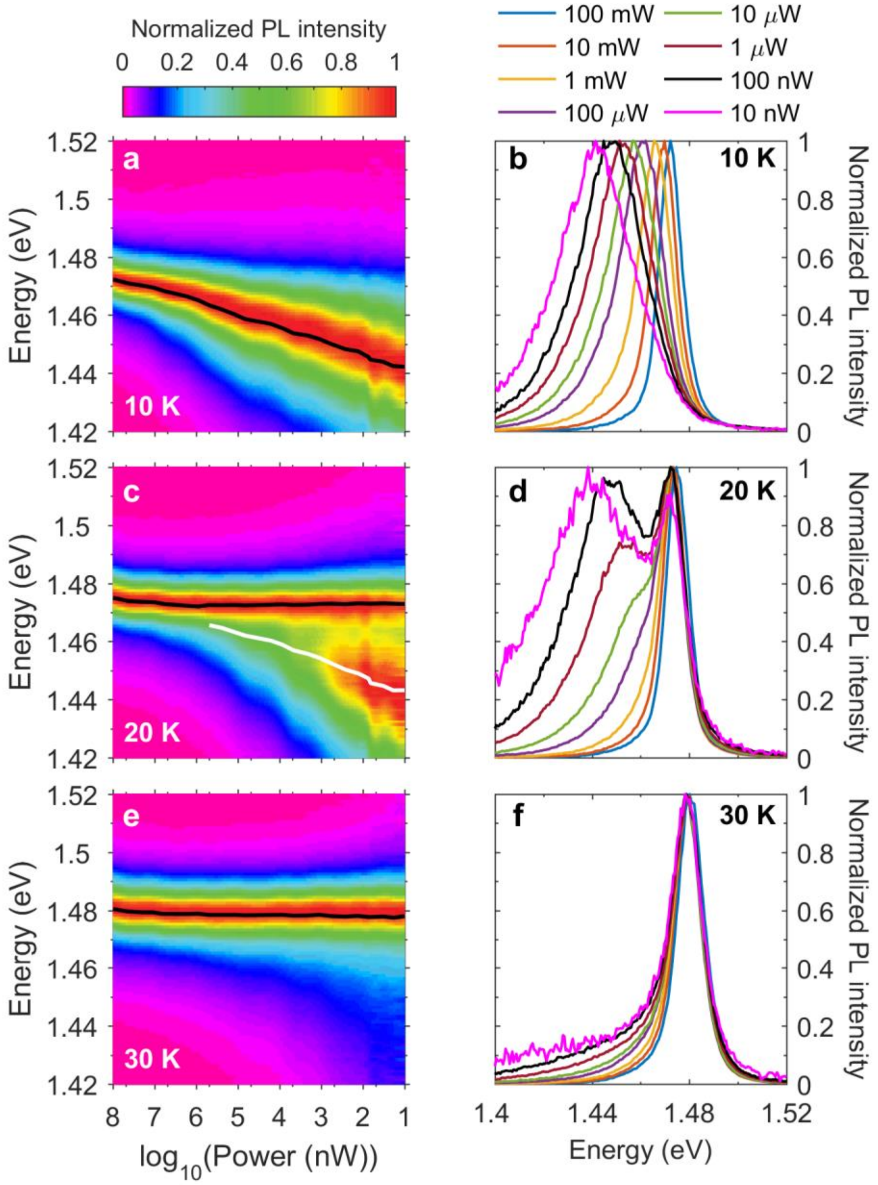

Figure S3. Color plots of the normalized steady-state PL spectra of $FAPbI_3$ at excitation powers between 10 nW and 100 mW, with selected spectra, at temperatures of **(a,b)** 10 K, **(c,d)** 20 K and **(e,f)** 30 K. The spectra were fitted with one or two Gaussian peaks, whose central energies are indicated by the solid black and white lines.

F. Rate equation model for anomalous relative Stokes shift

Li *et al.*[13] describe the rate of change of carrier population density $n(E,T,t)$ in localized states of energy E, at time t after excitation and at temperature T by the following rate equation:[13a]

$$\frac{\mathrm{d}n(E,T,t)}{\mathrm{d}t} = G(E,t) - \frac{n(E,T,t)}{\tau_\mathrm{r}} - n(E,T,t)\nu_\mathrm{e}e^{-(E_\mathrm{a}-E)/k_\mathrm{B}T} + \gamma_\mathrm{c}\frac{\rho(E)}{P}\lambda_\mathrm{a}(T,t). \tag{S15}$$

The first term on the right is the carrier generation rate, given by $G(E) = \kappa\,\rho(E)$, where κ is a constant of proportionality and $\rho(E)$ is the band tail density of states. The second term on the right describes the depopulation due to radiative recombination, which the carriers undergo with typical lifetime τ_r (higher-order recombination processes are neglected in this treatment). The third term on the right gives the rate of thermal escape to the unoccupied states above energy E_a, where ν_e is the attempt-to-escape rate. The final term represents the rate of carrier recapture at localized states, where λ_a is the rate at which carriers are thermally activated away from all the localized states, as given by

$$\lambda_\mathrm{a}(T) = \int_{-\infty}^{\infty} n(E',T)\nu_\mathrm{e}e^{-(E_\mathrm{a}-E')/k_\mathrm{B}T}\mathrm{d}E'. \tag{S16}$$

Some proportion (given by the recapture coefficient, λ_c) are recaptured by localized states, of which a fraction $\frac{\rho(E)}{P}$ are at energy E, where $P = \int_{-\infty}^{\infty}\rho(E')\,\mathrm{d}E'$. E_a is an energy below which the localized states are all occupied by carriers, analogous to the quasi-Fermi level of the localized state distribution.[13b]

Li *et al.* consider steady state $\left(\frac{\mathrm{d}n(E,T,t)}{\mathrm{d}t} = 0\right)$ conditions involving continuous carrier generation in order to derive the peak position of $n(E,T)$ at different temperatures, which represents the peak PL energy from the localized states. However, we measured PL under pulsed excitation conditions. The following treatment shows that the time-integrated PL peak has the same temperature dependence as in the steady-state case.

Under pulsed excitation, the time between pulses can be divided into two periods: δt, during which the excitation occurs, and Δt, which represents the rest of the pulsation period. We assume that δt is sufficiently short that all carrier generation occurs during this period, while the processes of recombination, thermal escape and recapture are confined to Δt. The net result of the three processes occurring during Δt is to remove all of the carriers generated in the localized states at energy E during δt, which can be expressed in the following equality:

$$N_\mathrm{generated}(E,T) = N_\mathrm{radiated}(E,T) + N_\mathrm{escaped}(E,T) - N_\mathrm{captured}(E,T) \tag{S17}$$

where N_x is the absolute value of the carrier population density added or removed from localized states of energy E by process x during the course of an excitation cycle.

Considering each term in Equation (S17) in turn:

$N_\mathrm{generated}(E,T) = \int_{\delta\mathrm{t}} G(E)\mathrm{d}t = \mu\,\rho(E)$, where μ is a constant of proportionality. (S18)

$$N_\mathrm{radiated}(E,T) = \frac{1}{\tau_\mathrm{r}}\int_{\Delta t} n(E,T,t)\,\mathrm{d}t \tag{S19}$$

$$N_\mathrm{escaped}(E,T) = \nu_\mathrm{e}e^{-(E_\mathrm{a}-E)/k_\mathrm{B}T}\int_{\Delta t} n(E,T,t)\,\mathrm{d}t \tag{S20}$$

$$N_{\mathrm{captured}}(E,T) = \int_{\Delta t} \gamma_c \lambda_{\mathrm{a}}(T,t)\gamma_{\mathrm{c}} \frac{\rho(E)}{P}\,\mathrm{d}t \qquad \text{(S21)}$$
$$= \gamma_{\mathrm{c}} \frac{\rho(E)}{P} \int_{-\infty}^{\infty} \nu_{\mathrm{e}} e^{-(\nu_{\mathrm{e}}-E')/k_{\mathrm{B}}T} \int_{\Delta t} n(E,T,t)\,\mathrm{d}t\,\mathrm{d}E'$$

Now let $m(E,T) = \int_{\Delta t} n(E,T,t)\,\mathrm{d}t$, which is the mean charge-carrier distribution over the period Δt, so Equation (S17) becomes

$$\mu\,\rho(E) = \left(\frac{1}{\tau_r} + \nu_{\mathrm{e}} e^{-(E_{\mathrm{a}}-E)/k_{\mathrm{B}}T}\right) m(E,T) - \gamma_{\mathrm{c}} \frac{\rho(E)}{P} \int_{-\infty}^{\infty} \nu_{\mathrm{e}} e^{-(E_{\mathrm{a}}-E')/k_{\mathrm{B}}T} m(E',T)\mathrm{d}E'$$
$$= \left(\frac{1}{\tau_r} + \nu_{\mathrm{e}} e^{-(E_{\mathrm{a}}-E)/k_{\mathrm{B}}T}\right) m(E,T) - \gamma_{\mathrm{c}} \frac{\rho(E)}{P} \lambda'(T) \qquad \text{(S22)}$$

Where $\lambda'(T)$ represents the total number of carriers which escaped from localized states over the course of Δt.Therefore, $m(E,T) = A(T)B(E,T)$, where

$$A(T) = \mu + \frac{\gamma_{\mathrm{c}}}{P}\lambda'(T)$$
$$B(E,T) = \frac{\rho(E)}{\frac{1}{\tau_{\mathrm{r}}} + \nu_{\mathrm{e}} e^{-(E_{\mathrm{a}}-E)/k_{\mathrm{B}}T}} \qquad \text{(S23)}$$

Since $A(T)$ is a function of T only, $B(E,T)$ describes the shape of the PL spectrum. This is the same result obtained for the steady-state, continuous excitation case by Li *et al.*. The peak of the spectrum occurs when $\partial B(E,T)/\partial E = 0$.

Li *et al.* consider the more involved case of a Gaussian density of states, but here we derive an expression for the peak energy for an exponential density of states (DOS) of the form $\rho(E) \propto e^{E/\varepsilon_0}$, where ε_0 represents the energy scale for the depth of the trap DOS. In this case, when $\partial B(E,T)/\partial E = 0$:

$$\frac{1}{\varepsilon_0}\left(e^{-(E_{\mathrm{a}}-E)/k_{\mathrm{B}}T} + \frac{1}{\nu_{\mathrm{e}}\tau_{\mathrm{r}}}\right) = \frac{1}{k_{\mathrm{B}}T} e^{-(E_{\mathrm{a}}-E)/k_{\mathrm{B}}T} \qquad \text{(S24)}$$

$$e^{-(E_{\mathrm{a}}-E)/k_{\mathrm{B}}T}\left(1 - \frac{\varepsilon_0}{k_{\mathrm{B}}T}\right) = -\frac{1}{\nu_{\mathrm{e}}\tau_{\mathrm{r}}} \qquad \text{(S25)}$$

$$E_{\mathrm{peak}} = E_{\mathrm{a}} + k_{\mathrm{B}}T \ln\left[\frac{1}{\nu_{\mathrm{e}}\tau_{\mathrm{r}}} \frac{k_{\mathrm{B}}T}{\varepsilon_0 - k_{\mathrm{B}}T}\right] \qquad \text{(S26)}$$

The model is divergent for $\varepsilon_0 \leq k_{\mathrm{B}}T$.

Table S1. Extracted band tail parameters for rate equation model. Fitted values of band tail depth (σ), filling level (E_{a}) and ratio of charge-carrier transfer and recombination timescales ($\nu_{\mathrm{e}}\tau_{\mathrm{r}}$). We assume $\nu_{\mathrm{e}}\tau_{\mathrm{r}}$ to be independent of excitation fluence and fix it at 10^5 in our fits, based on estimates of ν_{e} and τ_{r} being of the order of the Debye frequency[14] (~10^{12} s^{-1} for $\mathrm{MAPbI_3}$)[15], and inverse of the monomolecular rate constant (k_1 ~ 10^7 s^{-1} for $\mathrm{FAPbI_3}$)[16] respectively.

Fluence [nJ cm^{-2}]	ε_0 [meV]	E_{a} [meV]	$\nu_{\mathrm{e}}\tau_{\mathrm{r}}$
390	2.0	-0.7	*[10^5]*
110	2.0	-8.3	*[10^5]*
10	2.5	-16.5	*[10^5]*

G. **Monte Carlo model of the anomalous relative Stokes shift**

Baranovskii *et al.* simulate the relaxation of excitons within a distribution of localized states using a Monte Carlo technique.[17] We used the simulation algorithm described in Reference [17a], adapted for a three-dimensional material.

Within the simulation algorithm, the excitons are modelled as single particles moving between localized states, which are randomly distributed in a cube with sides of length $N_0^{1/3}$containing N_0 sites. The energies of the states are distributed according to the DOS of the band tail, which for an exponential density of states is

$$\rho(E) = \frac{N}{\varepsilon_0}\exp\left(\frac{E}{\varepsilon_0}\right) \tag{S27}$$

where ε_0 is the characteristic energy scale for the depth of the trap DOS, E is the trap energy (on a scale where the band edge is at E=0) and N is the concentration of localized states (1 per unit volume).

An exciton occupying site i (with energy E_i) can either recombine radiatively, with characteristic lifetime τ_r (assumed to be independent of temperature or E), or tunnel to an empty site j (with energy E_j) at distance r_{ij} according to the Miller-Abrahams tunnelling rate[18]

$$v_{ij} = v_e \exp\left(-\frac{2r_{ij}}{\alpha} - \frac{E_j - E_i + \left|E_j - E_i\right|}{2k_B T}\right) \tag{S28}$$

where ν_e is the attempt-to-escape frequency and α is the decay length of the localized exciton centre-of-mass wavefunction. Therefore, the total rate of escape from a given site i is $v_i = \frac{1}{\tau_r} + \sum_j v_{ij}$, where the summation index j runs over all possible hopping sites. Since ν_{ij} falls exponentially with distance and the difference in energy between sites, only the 32 largest terms in the sum were used in the computation.

Excitons are introduced one to the grid of sites at a time, starting from a random site. It is assumed that the charge-carrier density is sufficiently low that excitons relax independently. For an exciton at site i, a random number ξ_i from a uniform distribution between 0 and 1 is generated to determine the time $t_i{}^{-1} = -v_i \ln(\xi_i)$ until the exciton leaves the site. A second random number then determines whether this is by tunnelling to another site in the band tail, or by recombining. In the former case, t_i is added to the time counter, and the process repeated. In the latter case, the time and energy of the exciton at recombination are recorded, and a new exciton considered, until all n excitons have recombined.

The parameters of the model can be expressed as the dimensionless quantities $\nu_e\tau_r$, $N\alpha^3$ and k_BT/ε_0. $\nu_e\tau_r$ describes the degree to which hopping is faster than recombination, $N\alpha^3$ is the fraction of the volume per site which is occupied by the exciton wavefunction, and k_BT/ε_0 is the thermal energy normalized by the band tail depth.

For the simulations shown in Figure 3d of the main text, $\nu_e\tau_r = 10^5$ (as justified in Table S1), $N_0=35^3$ and $n=10^4$. The mean value of the PL energy was treated as the relative Stokes shift.[17a, 19]

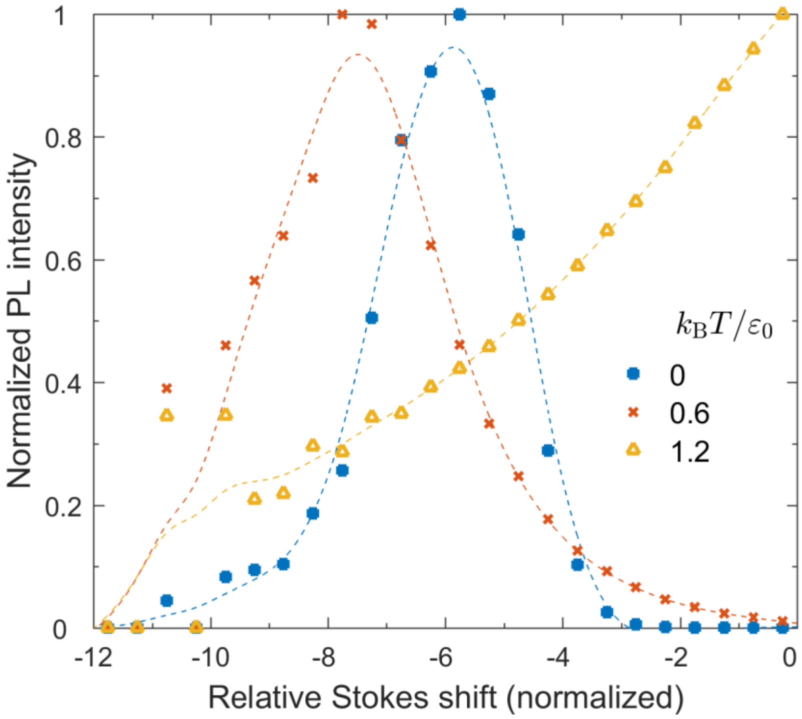

Figure S4. Temperature dependence of simulated band-tail PL spectra. PL spectra from Monte Carlo simulations of band-tail recombination at selected values of the normalized temperature $k_\mathrm{B}T/\varepsilon_0$, where T is the temperature and ε_0 is the inverse slope of the band tail. The dashed lines are a guide to the eye for the simulated spectra. The PL energy is expressed as a relative Stokes shift, normalized against ε_0. For these simulations, $N\alpha^3 = 0.25$, $\nu_e\tau_r = 10^5$, $N_0 = 35^3$ and $n=5 \times 10^5$.

H. Time and power dependence of PL at 100 K.

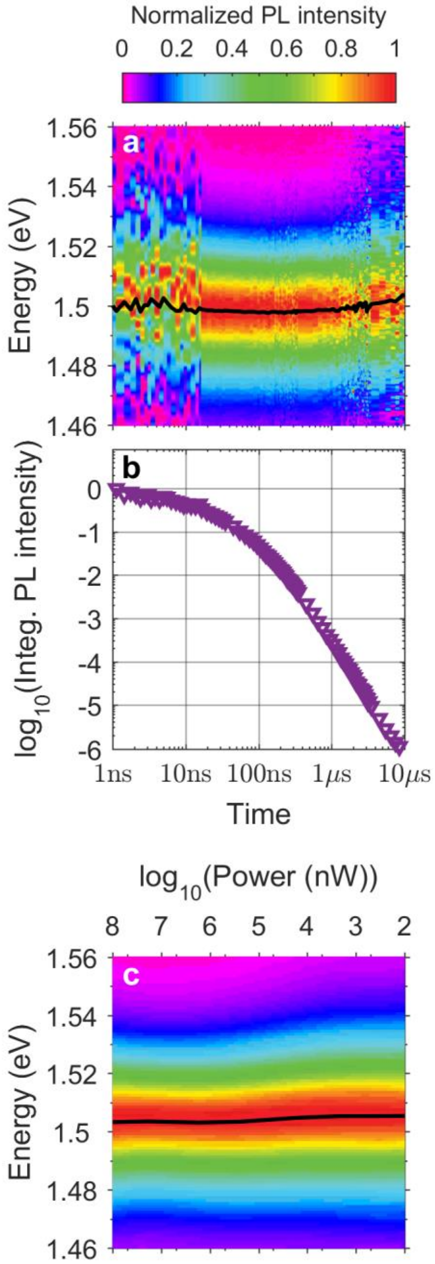

Figure S5. (a) Color plot of the normalized time-dependent PL spectra of FAPbI$_3$ at a temperature of 100 K and at times between 1 ns and 1 ms. **(b)** The corresponding spectrally integrated PL intensity transient. **(c)** Color plot of the normalized steady-state PL spectra of FAPbI$_3$ at a temperature of 100 K and excitation powers between 10 nW and 100 mW. In both color plots, the spectra were each fitted with a single Gaussian peak, whose central energies are indicated by the solid black line.

I. References

[1] M. B. Johnston, L. M. Herz, *Acc. Chem. Res.* **2016**, 49, 146.

[2] a) N. K. Noel, S. D. Stranks, A. Abate, C. Wehrenfennig, S. Guarnera, A. Haghighirad, A. Sadhanala, G. E. Eperon, S. K. Pathak, M. B. Johnston, A. Petrozza, L. Herz, H. Snaith, *Energ. Environ. Sci.* **2014**, 7, 3061; b) G. Xing, N. Mathews, S. Sun, S. S. Lim, Y. M. Lam, M. Grätzel, S. Mhaisalkar, T. C. Sum, *Science* **2013**, 342, 344.

[3] a) D. Shi, V. Adinolfi, R. Comin, M. Yuan, E. Alarousu, A. Buin, Y. Chen, S. Hoogland, A. Rothenberger, K. Katsiev, Y. Losovyj, X. Zhang, P. A. Dowben, O. F. Mohammed, E. H. Sargent, O. M. Bakr, *Science* **2015**, 347, 519; b) L. Wei, J. Peng, W. Weiying, M. Defeng, L. Guipeng, W. Zhanguo, W. Jiaming, X. Fujun, S. Bo, *J. Semicond.* **2014**, 35, 093001.

[4] a) D. W. DeQuilettes, S. M. Vorpahl, S. D. Stranks, H. Nagaoka, G. E. Eperon, M. E. Ziffer, H. J. Snaith, D. S. Ginger, *Science* **2015**, 348, 683; b) G. E. Eperon, S. D. Stranks, C. Menelaou, M. B. Johnston, L. M. Herz, H. J. Snaith, *Energ. Environ. Sci.* **2014**, 7, 982.

[5] X. Li, D. Bi, C. Yi, J.-D. Decoppet, J. Luo, S. M. Zakeeruddin, A. Hagfeldt, M. Gratzel, *Science* **2016**, 353, 58.

[6] a) O. Mülken, A. Blumen, T. Amthor, C. Giese, M. Reetz-Lamour, M. Weidemüller, *Phys. Rev. Lett.* **2007**, 99, 090601; b) J. Tilchin, D. N. Dirin, G. I. Maikov, A. Sashchiuk, M. V. Kovalenko, E. Lifshitz, *ACS Nano* **2016**, 10, 6363.

[7] a) D. J. Huntley, *J. Phys: Condens. Mat.* **2006**, 18, 1359; b) R. Saito, K. Murayama, *Solid State Commun.* **1987**, 63, 625.

[8] a) J. T. Randall, M. H. F. Wilkins, *Proc. R. Soc. London, Ser. A* **1945**, 184, 390; b) D. J. Dunstan, *Philos. Mag. B* **1982**, 46, 579; c) A. K. Jonscher, A. de Polignac, *J. Phys. C: Solid State Phys.* **1984**, 17, 6493; d) R. A. Street, *Adv. Phys.* **1981**, 30, 593.

[9] M. Kuno, D. P. Fromm, H. F. Hamann, A. Gallagher, D. J. Nesbitt, *J. Chem. Phys.* **2000**, 112, 3117.

[10] a) I. J. McNeil, D. L. Ashford, H. Luo, C. J. Fecko, *J. Phys. Chem. C* **2012**, 116, 15888; b) J. Orenstein, M. A. Kastner, *Solid State Commun.* **1981**, 40, 85.

[11] J. T. Randall, M. H. F. Wilkins, *Proc. R. Soc. London, Ser. A* **1945**, 184, 365.

[12] D. Monroe, *Phys. Rev. Lett.* **1985**, 54, 146.

[13] a) Q. Li, S. J. Xu, W. C. Cheng, M. H. Xie, S. Y. Tong, C. M. Che, H. Yang, *Appl. Phys. Lett.* **2001**, 79, 1810; b) Q. Li, S. J. Xu, M. H. Xie, S. Y. Tong, *Europhys Lett.* **2005**, 71, 994; c) Q. Li, S. J. Xu, M. H. Xie, S. Y. Tong, *J. Phys: Condens. Mat.* **2005**, 17, 4853.

[14] M. Baranowski, M. Latkowska, R. Kudrawiec, J. Misiewicz, *J. Phys: Condens. Mat.* **2011**, 23, 205804.

[15] N. Onoda-Yamamuro, T. Matsuo, H. Suga, *J. Phys. Chem. Solids* **1990**, 51, 1383.

[16] W. Rehman, R. L. Milot, G. E. Eperon, C. Wehrenfennig, J. L. Boland, H. J. Snaith, M. B. Johnston, L. M. Herz, *Adv. Mater.* **2015**, 27, 7938.

[17] a) S. Baranovskii, R. Eichmann, P. Thomas, *Phys. Rev. B* **1998**, 58, 13081; b) B. Dal Don, K. Kohary, E. Tsitsishvili, H. Kalt, S. D. Baranovskii, P. Thomas, *Phys. Rev. B* **2004**, 69, 045318.

[18] A. Miller, E. Abrahams, *Phys. Rev.* **1960**, 120, 745.

[19] O. Rubel, M. Galluppi, S. D. Baranovskii, K. Volz, L. Geelhaar, H. Riechert, P. Thomas, W. Stolz, *J. Appl. Phys.* **2005**, 98, 063518.